

# APPLICATION OF ION PROPULSION SYSTEM TO COMMUNICATIONS SATELLITES

F. Porte \*, P. Saint-Aubert \*, D. Mawby \*, J. Hsing\*\*

\* MATRA MARCONI SPACE \*\* INTELSAT Washington D.C.

## Abstract

To meet the ever increasing communications traffic demands, INTELSAT is exploring a number of technological solutions. One of these options is to take advantage of the high efficiency ion propulsion thrusters for reducing the launch mass of a large bandwidth communications satellite. Under an INTELSAT contract, MATRA MARCONI SPACE (MMS) carried out a study to identify candidate positioning and orientation systems (POS) superior to those using chemical systems and to define spacecraft concepts which take the largest benefits of the Ion Propulsion System (IPS). The class of spacecraft considered in the study is in the two tons dry mass range.

This paper describes an IPS based system consisting of four ion thrusters mounted on two two-degree of freedom thruster pointing mechanisms (TPM). They are located on the anti-earth side of the north and south panels in the pitch/yaw plane. The IPS is primarily used for North South Station Keeping (NSSK). Two daily maneuvers are needed at each orbit node. Only one thruster is operated during each maneuver so that only two power conditioning units are needed. With proper selection of the two maneuver times and durations, the orbit eccentricity can be tightly controlled. Task sharing between the IPS and the Chemical Propulsion System (CPS) in the various phases of the mission (transfer, longitude drift control, repositioning and end of life deorbiting) has been optimized. Preliminary design and analysis of the spacecraft bus subsystems are included in this paper as well as an evaluation of the overall benefits of the proposed concept on the communications mission.

## 1. Introduction

The status of development of electric propulsion technologies is now sufficiently advanced to be considered for use on commercial communications spacecraft. Among the various technologies available (arcjets, gridded ion thrusters, Hall thrusters), the gridded xenon ion thruster, which offers the highest specific impulse, has been considered in the study. Several gridded ion thruster designs with similar performances are under development. The UK-10 ion thruster which is currently under development at MMS and which will be flown on ARTEMIS, is the basis of the IPS proposed in this paper. However, many results presented below generally apply to gridded ion thrusters of similar performances. A similar study with the SPT-100 Hall thruster has also been conducted at MMS. The results are not included in this paper.

Due to their specific characteristics and the large potential benefits they offer, it is worth reconsidering the entire spacecraft design in order to take the largest advantage of the benefits offered by an IPS, while carefully taking into account the additional constraints related to the IPS.

The reference mission considered in the study is the INTELSAT VII-A mission (1800 kg spacecraft dry mass, 525 kg/3.6 KWe payload mass and power <sup>1</sup>). The study however applies more generally to large geostationary communications spacecraft of dry mass in the 1500 kg to 2000 kg dry mass range. The considered launchers are Ariane 4 (single launch) or Ariane 5 (dual launch) and Atlas 2AS.

## 2. UK-10 propulsion system description

An ion propulsion system consists of a high pressure xenon storage tank, pressure regulator, xenon flow controller and the ion thrusters and associated power conditioning units. The UK-10 propulsion system units are described in the following sections.

### 2.1 UK-10 ion thruster

#### 2.1.1 General description

The UK-10 is a gridded Kaufman xenon ion thruster of 10 cm diameter dished aperture which delivers 25 mN thrust at 3200 s specific impulse with a beam power of 500 W. The thruster was originally developed by DRA (UK) and has been industrialized by MMS. The UK-10 schematic is shown in figure 1. The thruster consists of a discharge chamber, a three-grid ion extraction system and a neutralizer.

A cylindrical drum forms the body of the discharge chamber. Inside the drum is a cylindrical anode. Inserted into the rear of the drum is the hollow cathode and its keeper, where electrons are generated by thermionic emission from a barium dispenser. The cathode is equipped with a heater to initialize the emission (cathode self-heating is sufficient in steady-state conditions). A disc-shaped baffle controls the plasma in the cathode vicinity. At the periphery of the discharge chamber are distributed six solenoids and inner and outer pole pieces for the magnetic circuit. Three xenon propellant flows are supplied to the thruster for neutralizer operation, cathode operation and main flow, the latter being introduced through a manifold located at the rear of the discharge chamber. Xenon is passed through the cathode in order to generate the initial arc between the cathode and the keeper caused by the Paschen breakdown of the gas. Electrons which have been removed from the cathode are

then attracted towards the positive potential of the anode and trapped in the magnetic field lines created by the solenoids and pole pieces until they collide with the xenon atoms in the main flow with sufficient energy to cause ionization. The ionization process has been optimized by design of the inner pole-baffle assembly and correct selection of the anode-to-keeper voltage.

The three-grid ion extraction system is fitted at the front of the discharge chamber. The inner or screen grid which maintains the discharge plasma is biased at a 1100 V potential which is also the reference potential of the discharge chamber (isolator tube sections are fitted at the gas inlets). The second grid, the accelerator grid, is set at a negative voltage (-250 V) causing ions to be extracted and accelerated. The third grid, which is set at -40 V, protects the accelerator grid from the back-sputtering of charge-exchange ions (low energy ions resulting from collisions between the high energy ions and neutrals) which are attracted by the negatively biased accelerator grid. By properly selecting the ion optics, the ions follow paths which cause them to miss the grids and exit at high speed, of the order of 40 km/s. The grids are dished inwards to maintain the ion optics with thermally expanded grids, contributing also to the low beam divergence (95% of the ion beam contained within a 13° half angle cone).

The neutralizer, which is a hollow cathode identical to the main discharge cathode, forms a plasma bridge allowing the ion beam to be globally neutralized and preventing spacecraft charging.

### 2.1.2 UK-10 control scheme

The UK-10 control scheme has been designed with the following objectives:

- Throttling capability to offer flexibility for a variety of missions. For example, the operation of the UK-10 on ARTEMIS is foreseen at 18 mN (instead of 25 mN nominal) due to system level power limitations.
- Optimal operation for maximum thruster life
- Minimum degree of sputtering (minimum impacts on spacecraft environment).

To achieve these objectives the UK-10 design offers the following flexibility:

- Independent adjustment capability of the three propellant flows via the use of solenoid valves (off-time modulated) instead of fixed flows.
- Adjustment of the magnetic field by using solenoids instead of permanent magnets.

The control scheme includes four active control loops. The first control loop maintains the beam current (i.e. the thrust) at a selectable value by adjustment of the main flow. The three other control loops are designed to maintain optimum operation conditions in order to maximize thruster life. Thruster life of a gridded ion thruster is essentially limited by grid erosion and cathode life. As already mentioned, grid erosion in flight conditions is partly due to back-sputtering of

charge-exchange ions which is dependent on the density of neutrals present in the beam, and then on propellant utilization efficiency. The active control of the propellant utilization efficiency to a fixed value (>80%) both limits the grid erosion and guarantees stable operation over the thruster life. This is obtained via a second control loop which monitors the anode to keeper voltage and maintains it at a fixed predetermined value by adjustment of the solenoid current, i.e. magnetic field, thereby realizing an adjustable plasma impedance.

Cathode life, which is strongly dependent on its operating temperature, is maximized via a third control loop which maintains the keeper voltage at its nominal value by adjustment of the cathode xenon flow, leading to constant temperature conditions over the cathode life. The same control loop is applied to the neutralizer operation.

This control approach both maximizes the thruster life and establishes repeatable operating conditions leading to a more deterministic behaviour of the thruster than an "open loop" design. Although the system complexity and mass is slightly increased (additional flow control valves and drivers, adjustable solenoid supply), these effects are considered outweighed by the benefits of flexible and optimal operation for thruster life maximization.

### 2.2 Power conditioning and control equipment (PCCE)

The equipment, which requires 750 W input power and weighs 12.3 kg, includes the following units:

Command and data gathering unit (CDGU) The CDGU, which includes a 1750 microprocessor unit, performs the control and monitoring tasks over the entire equipment and interfaces with the spacecraft data handling computer via an OBDH bus interface. It includes the PSME isolation, start valve drivers and the digitally driven regulation valve drivers.

Neutralizer and auxiliary power unit (NAPU): The ground-referenced NAPU includes the CDGU power converter, the neutralizer keeper (and trigger) and heater supplies.

Beam supply unit (BSU) The BSU which maintains the screen grid and accelerator grid to neutralizer return voltage at 1100 V and -350 V respectively, is the main PCCE supply.

Discharge power unit (DPU) The beam-referenced DPU provides the supplies to the anode, magnet, main cathode keeper (and trigger) and to the main cathode heater.

Electronic pressure regulator electronics (EPRE) This unit which is physically implemented in the PCCE is electrically independent of the other units. It performs the control and the monitoring of the PSDE (isolation and regulation valve drivers, pressure regulation) and includes its own converter section.

### 2.3 Propellant supply and monitoring equipment (PSME)

The PSME performs the function of controlling the three xenon flows necessary for thruster operation. The schematic of the unit is presented in figure 2. It consists of an isolation valve, three regulation valves, two start valves, three plenum

chambers and orifices, two temperature sensors and two valve heaters. During thruster operation each of the three regulator solenoid valves is separately actuated at a duty cycle corresponding to the required flow rate as determined by the CDGU software. The three plenum chambers are used to smooth out the xenon flow to an acceptable ripple level (lower than 1%). The start valves which bypass the cathode and neutralizer gas supply lines are pulsed on briefly to initialize the respective hollow cathode discharges through Paschen breakdown.

#### **2.4 Propellant storage and distribution equipment (PSDE)**

The PSDE schematic is presented in figure 3. It consists of two titanium spherical xenon storage tanks of 20 liters each where xenon is stored at 1.5 kg/liter (75 bars at 20°C), isolation and regulator valves, fill and drain valves, pressure and temperature transducers, valve heaters and an oxygen absorber which protects the cathodes from contamination by the air and provides a volume for pressure smooth out.

#### **3. CPS-IPS task sharing**

The use of IPS in all the mission phases has been thoroughly investigated in order to derive the optimum task sharing between the CPS and the IPS. The gain obtained by performing a given function with IPS must clearly be traded-off with the related increase of system complexity.

#### **3.1 Mission requirements**

The selection of the type of stabilization (spin or three-axis) during apogee firing has large impacts on many aspects of the spacecraft definition. If the spacecraft is passively spin stabilized, the moment of inertia (MOI) about the spin axis must remain maximum during the entire apogee maneuvers (minimum energy state condition). This situation leads to a limitation of the spacecraft height while the other dimensions are constrained by the minimum fairing diameter of the considered launchers. The use of IPS for station-keeping makes this issue even more problematic since the on-station propellant, which is considerably reduced, provides a much less substantial MOI contribution than would be the case with an optimized tank configuration in a conventional spacecraft design using chemical propulsion alone. Passive spin stabilization is therefore not consistent with the opportunity offered by IPS to significantly increase the payload range that can be launched with the existing launchers and has therefore not been selected in the study.

Active spin stabilization results in minimum spacecraft height limitations (the MOI about the spin axis must remain minimum during the entire apogee maneuvers) and may be not applicable for smaller missions. Furthermore the propellant consumption resulting from active nutation damping may become significant in multi-burn orbit insertion strategies (of typically one week transfer duration) as commonly used with restartable apogee engines.

Three-axis stabilization during apogee firing appears to be the best approach for an IPS equipped spacecraft of the considered mission range and has therefore been selected in

the study. Reference <sup>2</sup> presents the MMS patented three-axis transfer sequence successfully flown on ITALSAT.

This stabilization mode leads to a Reaction Control Thruster (RCT) configuration which provides torques about all three axes with redundancy and with sufficient control authority to compensate the disturbance torques during main engine firing.

The POS functions consist of attitude acquisitions in transfer orbit, orbit insertion maneuvers, on-station attitude acquisition, earth pointing, station-keeping (+/- 0.05° NSSK and EWSK), repositioning (30 m/s) and deorbiting (6 m/s).

#### **3.2 Orbit insertion**

Investigation of orbit insertion strategies involving the use of IPS has been performed in the first phase of this study and has been reported in reference <sup>3</sup>. The main results are summarized in this section.

The optimum strategy (i.e. which maximizes the achievable Beginning of Life (BOL) spacecraft mass by a given launcher) with IPS has been found to consist in separating the spacecraft on a subsynchronous transfer orbit, in circularizing the orbit with the chemical main engine at this subsynchronous altitude with simultaneous correction of most of the orbit inclination. The IPS is then continuously operated on a quasi-circular orbit with increasing radius up to geosynchronous orbit. The residual inclination (after chemical main engine firing) is removed during IPS operation by rotating the spacecraft about the earth line in order to create out-of-plane thrust components. For Kennedy launches (27° Geostationary Transfer Orbit (GTO) inclination) the above strategy is improved by operating the IPS on an elliptical orbit which is more favourable for inclination correction.

Given the available power in this flight phase (fully deployed solar array, payload switched-off, replacement heaters on), the thrust (100 mN for the reference mission) that can be achieved with the IPS can be derived (it is assumed that the solar array is sized for on-station conditions). For a given launcher the achievable BOL spacecraft mass can be established as a function of the orbit raising duration. Figure 4. presents the BOL mass gains with respect to a conventional strategy for Ariane 44L and Atlas 2AS and for orbit raising duration up to 250 days. The mass gains are significant since they reach 310 kg and 180 kg for a six-month transfer on Ariane and Atlas respectively. Using IPS for orbit raising has some impacts on the spacecraft design so that the above mass gains are effectively slightly reduced. These impacts have been taken into account in the evaluation.

The mass gains can be translated in launch cost saving by considering that a given spacecraft could be launched by a less powerful launcher or launcher version (a launch cost rate of 30 k\$ per launched kg in standard Ariane GTO has been assumed). With these assumptions the launch cost can be reduced by 14 M\$ on Ariane and by 9 M\$ on Atlas with a six-month orbit raising duration.

However this launch cost saving must be traded with the time delay on the beginning of the spacecraft operational life. The latter cost can be estimated by considering that the total investment (spacecraft and launch costs) is non-productive for the duration of the orbit raising (no revenue for the spacecraft operator). Considering a 100 M\$ spacecraft with a 100 M\$ launch cost and assuming a 1% monthly interest rate, the cost of the six-month delay would be 12 M\$. The overall benefits become then moderate on Ariane and negative on Atlas. Obviously this result is very sensitive to the assumed interest rate.

With the assumptions mentioned before, it has been concluded that IPS cannot be used in a general manner to reduce the deployment cost of geostationary communications spacecraft, the reason being that the achieved launch cost reduction just compensate for the cost related with the delay of the beginning of operational life. However, used in a less extensive way (i.e. shorter transfer duration) it can be used to offer flexibility in optimizing a given mission. Furthermore the useful payload launch capacity of the existing launchers can be significantly extended. This application may be interesting for certain missions which could not be launched with a conventional strategy.

Since this application is not general, the capability of orbit raising with IPS has not been maintained as a mandatory requirement in the following of the study.

### 3.3 North-South station-keeping (NSSK)

NSSK requires a mean yearly velocity increment of 46 m/s and is thus the most propellant consuming on-station function. It is clearly the main application of IPS and allows a launch mass reduction in the range of 700 kg (Ariane launch) for a 1800 kg dry mass spacecraft. This function is best entirely performed with IPS.

Taking into account typical spacecraft configuration constraints (solar array), orbital coupling and attitude control considerations, two generic ion thruster configurations can be derived.

In the first configuration (denoted 1, cf. figure 5.(a)), two ion thrusters are implemented on the anti-earth side of the North and South panels. Each ion thruster is oriented towards the nominal spacecraft centre of mass in order to minimize the disturbance torques during IPS operation, resulting in a typical 45° thrust orientation within the pitch/yaw plane. During a maneuver only one thruster is operated. The radial thrust component creates eccentricity and mean longitude shift. The impact on eccentricity is cancelled by breaking the NSSK maneuver in two maneuvers performed at each orbit node (cf. figure 6.(a)). The longitude shift which is generated by each daily maneuver makes the spacecraft drift. This drift is compensated by placing the spacecraft at a slightly higher altitude (about 400 m). Redundancy considerations lead to implement two more ion thrusters resulting in a 4-thruster configuration organized in two modules. A similar ion thruster arrangement was used on ATS 6 (cf. reference 4).

In the second configuration (denoted 2.1, cf. figure 5.(b)), two ion thrusters are symmetrically implemented on the North (or South) panel and canted outwards in order to avoid plume effects with the deployed solar array. Simultaneous firing of the two ion thrusters creates pure force (nominally torque free) along the North-South direction. One NSSK maneuver per day is performed. Redundancy is obtained by adding another ion thruster pair on the same or on the opposite North-South panel resulting also in a 4-thruster configuration.

### 3.4 East-West station-keeping (EWSK)

This task which includes longitude drift and orbit eccentricity control leads for the considered spacecraft range to a yearly velocity increment requirement of 2.8 m/s typically. The various ways of adding thrusters and power conditioning units to fulfill the entire EWSK function with full redundancy have been analysed. It has been found that the corresponding propellant mass savings is offset by the mass and cost of the additional hardware. The optimal approach consists then in taking maximum benefit of the two configurations presented before. Their capability to perform EWSK, at least partially, is now discussed.

*Configuration 1* Eccentricity control can be performed by taking advantage of the radial thrust component. The use of different firing durations between North and South maneuvers (cf. figure 6.(b)) offers an eccentricity correction capability for one direction of the apside line. Eccentricity correction along the other direction can be obtained by slightly shifting (12° maximum) the location of the North-South maneuvers, as indicated in figure 6.(c). A significant advantage of this approach is the minimal impact on the IPS utilization with respect to a pure NSSK strategy (same on-off cycling, total required ion thruster impulse increased by less than 2%) leading to no adverse impacts on thruster life. Orbit eccentricity can be virtually controlled to a zero value with negligible impact on Xenon mass budget leading to a significant reduction of the EWSK window with respect to conventional strategies using chemical propulsion. Longitude drift cannot be controlled with this configuration which does not provide any thrust component along the spacecraft velocity direction (in the case of a single location service, e.g. direct broadcasting, the thrusters could be implemented in a plane slightly offset with respect to the pitch-yaw plane in order to generate the thrust component along the spacecraft velocity axis necessary to compensate the local longitude acceleration; however this situation is not general and has not been considered in the following). This function is then realized with chemical thrusters. The corresponding yearly velocity increment, which depends upon the local longitude acceleration, varies from theoretically zero at the four equilibrium longitude stations (76°E, 172°E, 11°W, 105°W) up to the maximal value of 2 m/s at 117°E. The latter longitude station (worst case) has been considered in the propellant budget. This EWSK strategy leads then to chemical propellant mass savings since the yearly velocity increment of 2.8 m/s resulting from conventional EWSK strategies is reduced to a maximum of 2 m/s.

**Configuration 2.1** EWSK can be performed by taking benefit of the thrust component in the spacecraft velocity direction provided by this configuration. This is realized by firing a North and a South thruster of the east (or west) panel. In case of ion thruster failure, the maneuver involving the failed thruster is overtaken by chemical thrusters which necessitates the corresponding chemical propellant provision.

**Configuration 2.2** Another approach consists in selecting the ion thruster cant angle such that the thruster axis is directed towards the spacecraft centre of mass. EWSK maneuvers are performed by firing a single thruster of the east (or west) panel. This configuration offers a full station-keeping capability with redundancy. However the NSSK thrust efficiency is significantly reduced with respect to configuration 2.1, to less than 70% typically (instead of about 90%). The thrust component in the North-South direction generated during EWSK maneuvers slightly couples the EW and NS spacecraft motions.

This approach leads to a significant increase of the ion thruster impulse requirement. In order to minimize the number of ion thruster on-off cycles, the station-keeping scheme consists in skipping a NSSK maneuver every 10 days typically and to perform instead two EWSK maneuvers which simultaneously remove the longitude drift and orbit eccentricity built-up. This configuration which is slightly different to the configuration 2.1 is denoted 2.2 in the following.

### 3.5 Repositioning and deorbiting

INTELSAT's requirement regarding the repositioning capability is expressed as a 30 m/s provision when realized with chemical propulsion. This section discusses the benefits of performing this function with IPS.

The repositioning maneuver using IPS consists in a first phase where longitude drift towards the new location is built-up and in a second phase where the longitude drift is removed. In the two phases the IPS is continuously operated to generate thrust along the spacecraft velocity direction (no coast phase is assumed in order to minimize the repositioning duration). During the maneuver the power available to the IPS must be maximal. The payload is then switched-off with replacement heaters on leading to sufficient power for the operation of two UK-10 (the available power is significantly lower than during the orbit raising phase as a result of the solar array degradations when exposed to radiation in geostationary orbit).

In configuration 1 thrust along the spacecraft velocity direction with an efficiency of 70% is obtained by pitching the spacecraft by 90 degrees and by firing a North and a South thruster. In configuration 2.1 and 2.2 it is obtained by firing two thrusters of the same east (or west) panel. Under these conditions the repositioning duration and the Xenon consumption can be expressed as a function of the longitude difference between initial and final location.

The velocity increment of the same repositioning maneuver (same longitude change and same duration) performed with chemical propulsion (impulse maneuvers) can be computed

as well as the corresponding chemical propellant consumption.

Table 1 presents the duration and the propellant requirements of repositioning maneuvers for different longitude changes performed with IPS and CPS.

INTELSAT's requirement of 30 m/s which is equivalent to three repositioning maneuvers of 47° (or two repositioning maneuvers of 105°) of table 3 leads to a consumption of 25.2 kg of chemical propellant or of 11 kg of Xenon. Performing repositioning maneuvers with IPS would then lead to launch mass savings in the range of 26 kg. The main drawbacks are the additional requirement on ion thruster life (+ 20%) and the loss of flexibility to quickly relocate

Longitude change	180°	105°	47°	11.5°
IPS durations (days)	52	40	27	13
mean drift (°/day)	3.5	2.6	1.8	0.9
Xenon mass (kg)	7.2	5.5	3.7	1.8
CPS ΔV (m/s)	19.7	15.0	10.0	5.0
Propellant mass (kg)	16.5	12.6	8.4	4.2

**Table 1: Repositioning with IPS and CPS**

the spacecraft (e.g. to minimize service interruption in case of spacecraft failure at another location) due to the low thrust delivered by the IPS. The mass benefit being relatively modest, repositioning with IPS has not been selected. Repositioning is assumed in the following to be performed with chemical thrusters.

At end of life the spacecraft performs maneuvers with chemical thrusters to reach the higher altitude (+ 200 km) graveyard orbit with a propellant consumption of 5.4 kg typically. The same orbit can be achieved by operating the IPS during 115 hours with a 0.7 kg Xenon consumption. The corresponding launch mass savings (9 kg) does not justify the related operational complexity.

### 3.6 Attitude control during IPS operation

Disturbance torques during IPS operation appear when the thrust is not exactly aligned with the spacecraft centre of mass (c.m.). This mainly results from thrust vector misalignment within the thruster mechanical axes (1°), from uncertainties on the location of the spacecraft c.m. and on the c.m. excursion (solar array rotation, stored propellant). The resulting disturbance torques lie in the 10<sup>-3</sup> Nm range. These torques can be compensated with RCT (solar sailing or magnetic torquing do not provide the required torque level), cancelled by adjustment of the spacecraft c.m. location or by thruster gimbaling (and throttling in configuration 2.1).

In a fixed momentum Attitude Determination and Control Subsystem (ADCS), the use of RCT's, which need to be operated at their minimum impulse bit to maintain acceptable pointing performances, leads to a large number of thruster actuations exceeding the qualification range of existing bipropellant thrusters. In a 2-Degree of Freedom (2 DOF) momentum ADCS, the number of actuations is significantly reduced. The large associated propellant consumption leads however to a significant reduction of the launch mass savings (in the range of 100 kg with the above

assumptions). Obviously this consumption directly depends on the ion thrust misalignment which results in a poor robustness with respect to a poorly known parameter. Furthermore the chemical propulsion system is frequently activated. This approach which significantly reduces the benefits of using an IPS has not been selected.

The solar array is a significant contributor of the spacecraft c.m. excursion via the misalignment of its rotation axis and the thermo-elastic bending of the wing. It has been proposed<sup>5</sup> to use a solar array drive mechanism consisting of two series mounted rotary stepper motors with slightly biased rotation axes, thereby providing a vernier adjustment capability of the spacecraft c.m. location in the X-Z plane. Roll and yaw torques are compensated during the maneuver, while pitch momentum is stored and removed during normal operation using solar pressure effect on the wing. This approach has not been selected because of its hardware and operational complexity (different solar array orientations between normal operation and maneuvers) and is not adapted to low specific power payloads like INTELSAT missions (medium power solar arrays, massive spacecraft).

The selected approach consists in using two-axis (configuration 1 and 2.2) or one-axis (configuration 2.1) TPM's as described in section 5.2.2.

#### 4. Selection of the POS concept

This section reports the evaluation of the three thruster configurations described before according to the following criteria:

- (i) IPS dry mass budget
- (ii) On-station propellant budget (xenon and chemical propellant)
- (iii) IPS recurring costs
- (iv) IPS reliability and qualification requirements
- (v) Station-keeping performances and operational load
- (vi) Impacts on spacecraft design (Power, Thermal, ADCS)
- (vii) System issues (Electromagnetic Interference (EMI), contamination)

Table 2 presents the ranking of the three configurations. Criteria (i) to (iii) have been synthesized under one item since dry mass and on-station propellant budget can be translated in launch mass and in turn launch cost, which added to the IPS recurring cost leads to the overall system cost.

Configuration 1 requires only two PCCE's (nominal and redundant units), one unit operating alternatively one North and one South thruster, as will be developed in section 5.1. Configurations 2.1 and 2.2 require four PCCE's (redundancy included) since two thrusters are operated simultaneously. The IPS dry mass and cost is then significantly higher in configurations 2.1 and 2.2 than in configuration 1. The counterpart of configuration 1 is the relatively modest NSSK thrust efficiency (70% instead of 90% in configuration 2.1) which increases by 29% the ion thruster qualification

requirement (the impact on propellant budget is low due to the high thruster specific impulse). Due to its EWSK capability and in spite of its 70% NSSK thrust efficiency, configuration 2.2 improves the performance of configuration 2.1 in terms of system benefit.

	Conf. 1	Conf 2.1	Conf 2.2
System benefits	1	3	2
Reliability	1	2	3
Qual. requirement	2	1	3
NSSK	yes	yes	yes
EWSK	yes	partial	yes
Eccentricity		partial	
Drift	no	partial	yes
SK accuracy/autonomy	1	2	2
Impacts on S/C design			
ADCS	1	1	2
Power/Thermal	1	2	3
System issues	1	2	3

**Table 2: Ion thruster configuration evaluation**

The impacts on the power subsystem have been thoroughly investigated in each configuration. At solstice the use of the battery on the hot radiator side (which receives solar flux) is prohibited for thermal reasons. In order to limit the depth of discharge (DoD) of the other battery to an acceptable value and to recharge the battery after the maneuver, the solar array power requirement at solstice is increased. This additional power requirement can reach up to 10% of the total solar array power for an INTELSAT VII-A mission in configuration 2.1 (even more in configuration 2.2) and 2% in configuration 1 where the maneuvers are executed at each node. Configuration 1 also minimizes the load on the batteries and the radiator areas allocated to the PCCE thermal control.

Finally, configuration 1 maximizes the system benefits offered by the IPS, has the best reliability (only one PCCE is necessary to operate a thruster branch), leads to minimum impacts on the spacecraft design especially relating to power and thermal and minimizes the North-South to East-West orbital coupling (better station-keeping accuracy, larger autonomy). Since in configuration 1 no antenna is located in the ion thruster half space (the ion beam and radio-frequency signal path are fully decoupled, antenna reflectors free of thruster contamination) and since the ion beam to solar array geometric separation is higher, this configuration is expected to be the most favourable one with respect to system issues as EMI, erosion and contamination of spacecraft surfaces.

All these considerations have led to the selection of configuration 1.

## 5. Spacecraft concept description

### 5.1 IPS

The schematic of the IPS is presented in figure 7. The subsystem is organized in two redundant branches consisting each of one North thruster and one South thruster, two PSME's, one PCCE and one thruster switching electronics (TSE). The MMS patented connection scheme is the following. The non-resistive lines (beam supply, anode

supply, cathodes supplies) are permanently connected to both thrusters via a "Y" harness since no current flows through the non-operating thruster when the plasma discharge is absent. The resistive lines (heaters, magnet supply, valve drivers) can be routed to one or the other thruster and PSME via relays implemented in the TSE. The relays associated to beam-referenced lines are entirely biased to the beam voltage and are therefore not submitted to high voltage differences between their connections. This approach avoids the use of relays with high voltage isolation requirements.

The reliability of the IPS has been assessed to 0.958 at 15 years which is comparable to the reliability of state-of-the-art CPS (the reliability contribution of the latter being now considerably reduced since the CPS is hardly used on station).

## **5.2 ADCS**

### **5.2.1 Yaw sensing concept**

The necessity of full three-axis attitude reference including yaw during the long duration NSSK maneuvers is a new requirement on the ADCS. The NSSK maneuvers are performed close to a line normal to the vernal axis. The drift maneuvers can be performed in two symmetric maneuvers anywhere on the orbit and preferably at 6 a.m./6 p.m. local time. With these considerations sufficient earth to sun separation (as seen from the spacecraft) is available during all maneuvers all over the year so that the sun can be used as yaw reference.

If the sun reference is used as absolute yaw reference, the sun sensor must be accurate (sensor error amplified via geometric decoupling coefficients) and must be implemented on stable locations against thermal distortions. The field of view must also be free of appendages such as antenna reflectors. This necessitates the use of several accurate sun sensors distributed on the spacecraft body and thus to a complex determination system.

The use of the sun as relative yaw reference (as a gyro) decreases the accuracy requirement of the sun sensor so that a simple analog sun sensor can be used. Regarding thermo-elastic distortions, only stability over the maneuver duration is relevant. The sensor can therefore be implemented on the solar array which is submitted to significant thermal bending but whose thermal environment is stable since permanently facing the sun. The proposed concept consists of two two-axis analog sun sensors mounted on each solar array wing associated to an on-board momentum provided by a wheel. The accuracy of this concept and the algorithms (calibration, observer) to be used have been investigated, supported by EUROSTAR spacecraft flight results, using the telemetered solar array tracking loop sun sensor data. The analysis has shown that a yaw accuracy of  $0.20^\circ$  can be obtained with this concept, which is consistent with the antenna pointing accuracy of a typical communications mission.

### **5.2.2 ADCS architecture**

The special features of the proposed ADCS architecture are the following:

- Relative yaw determination with solar array mounted sun sensors.
- 2 DOF bias momentum providing gyroscopic stiffness and three-axis momentum exchange capability used to control the spacecraft in all operational modes.
- EUROSTAR type solar array flaps for compensation of the inertial disturbance torques in normal operation (constant orientation with respect to the sun).
- TPM's which cancel the disturbance torques during NSSK maneuvers.
- Use of RCT during the drift maneuvers (series of pulses) at 6 a.m./6 p.m. and for pitch desaturation.

The orientation commanded to the TPM's is such that no angular momentum is stored in the 2 DOF system during a maneuver. The design is tolerant of a single TPM failure, e.g. failure to delatch a TPM. In this case, the disturbance torques during the maneuver, where the corresponding ion thruster is active, is stored in the 2 DOF system and removed during the next maneuver involving the opposite thruster. The proposed utilization does not require large cycling of the TPM.

The momentum accumulated during normal operation due to inertial disturbance torques could be removed during the NSSK maneuvers by proper orientation of the TPM but would lead to larger orbital coupling. The use of EUROSTAR solar array flaps has therefore been preferred.

The 2 DOF system can be realized in the three following ways in decreasing order of heritage:

- Four wheel configuration: two "V" momentum wheels in the pitch-yaw plane and two reaction wheels in the roll-yaw plane in a 3 among 4 redundancy scheme.
- Two momentum wheels mounted in a common (or separated) gimbal platform.
- Two magnetic bearing wheels MW-X with two-axis gimbal capability ( $\pm 1.7^\circ$ ) currently under development at TELDIX 6.

These systems lead to similar recurring costs but the MW-X minimizes the mass and the power consumption, offers high reliability (especially when compared to the four-wheel configuration) and facilitates the accommodation on the spacecraft. Furthermore since there is no limitation upon the number of gimbal actuations, it can be used in an extensive manner. This promising wheel has therefore been selected in the study.

The performance of the proposed ADCS has been analysed. The overall antenna pointing accuracy is improved by  $0.02^\circ$  with respect to conventional design (with CPS), allowing a better optimisation of the antenna performance particularly relevant when high directivity is required.

### **5.3 Station-keeping strategy and operational aspects**

The main features of the station-keeping strategy are:

- Compensation of the secular inclination drift only.

- Combined inclination/eccentricity control.
- Drift control using RCT pulses triggered at 6a.m./6p.m. once every three to four days typically.

Task sharing between the spacecraft computer unit (SCU) and the spacecraft operation centre (SOC) is the following: spacecraft tracking is performed by the SOC at regular interval, typically once every two weeks. The updated orbital data are then used to compute the maneuver parameters of the next two weeks, which are then uploaded within the SCU and automatically executed in due time.

The performance of the strategy has been analysed using precise orbital models and taking into account the various sources of errors, namely the shift of the spacecraft centre of mass, yaw error, thrust level uncertainty. The effect of the constant and slowly varying errors can be identified after a calibration phase and compensated by adjustment of the maneuver parameters. Only the non-repeatable part of these errors impacts the station-keeping window. Figure 8 presents the mean longitude evolution over a two-week period after calibration of the repeatable orbital coupling effects and considering the non-repeatable errors as systematic errors over the two-week period (worst case assumption). The spacecraft has drifted by less than  $0.007^\circ$ . The allocation for eccentricity, which is very tightly controlled according to the combined inclination-eccentricity control scheme, is very low. The analysis of all error contributions shows that, if spacecraft tracking is performed once every two weeks and with the above pessimistic assumptions, the spacecraft can then be controlled within a station-keeping window of  $\pm 0.02^\circ$ .

The advantage of this strategy can be used either to control the spacecraft within a very tight EWSK window in order to collocate several spacecraft in a  $\pm 0.05^\circ$  slot or to significantly increase the spacecraft autonomy depending on the spacecraft operator requirements.

## **5.4 Power**

### **5.4.1 General**

In the following the power subsystem topology is assumed to be a fully regulated single bus system. All the available solar array power is then routed to the IPS during NSSK maneuvers. The battery provides the complement, when necessary (at end of life), and is recharged after the maneuver. This approach which takes advantage of the higher solar array efficiency during the early part of the life, both minimizes the battery cycling and the solar array power requirements.

If the subsystem is semi-regulated, the PCCE's are connected to the batteries via "Y" diodes so that the power load is equally distributed to each battery (connection to the power bus would lead to drop the bus voltage during the maneuver down to the battery voltage and would lead to operate the solar array at a non-optimum voltage resulting in higher battery DoD). In order to minimize the battery DoD, the available solar array power is routed to the PCCE during NSSK maneuvers via the use of high power chargers.

As already mentioned, the hot battery cannot be used at solstice. It must therefore be possible to maintain either battery in trickle charge while the other is operating.

### **5.4.2 Battery thermal control**

Since the hot battery is not used at solstice, the hot case occurs at equinox where IPS operation is superimposed to spacecraft operation during eclipses. The battery cycle will consist of the main discharge, the first recharge, the first maneuver (138 mn maximum duration), the second recharge, the second maneuver, the third recharge and the trickle charge before the new eclipse. In order to limit the maximum cell temperature at the end of the main discharge, the battery radiator area needs to be increased by 25% with respect to case without IPS, and in addition the heater power activated in the first (endothermal) part of the recharge.

### **5.4.3 Solar array sizing**

IPS operation leads to new power requirements. At solstice the active battery must be recharged before the next maneuver leading to 2 % additional solar array power requirement. During the maneuver this power is used to support the battery, contributing to minimize the DoD (40 % at end of life). At equinox the charge power must be sufficient to return the energy drawn from the batteries during the eclipse and the NSSK maneuvers with sufficient time between the end of charge and the next eclipse to insure acceptable cell temperature at eclipse entry. The resulting additional power requirement has been assessed to 3 %.

Since the equinox is the sizing case in most missions (due to battery charge and heater power), the impact on the solar array sizing is assessed to 3% power increase with respect to a mission without IPS.

### **5.4.4 Battery cycling**

The battery cycling with and without IPS are presented in figure 9 taking into account the long term solar array degradations and the seasonal variations (solar flux, cell temperature). For simplification it has been assumed that only one battery is used during NSSK maneuvers outside the eclipse season although both batteries can still be used as long as the hot battery temperature is acceptable. At the beginning of life the power delivered by the solar array is sufficient to entirely supply the IPS. As the efficiency of the solar array decreases, the battery DoD increases up to 40% at end of life.

In order to assess the criticality with respect to battery ageing, the additional cycling imposed to the batteries as a result of the IPS operation has been compared to battery life test data. Reference <sup>7</sup> presents a recent (1991) compilation of Nickel Hydrogen cell life test data. An envelope of these data presented in figure 10 has been used in the following and clearly shows that the lower the DoD, the larger the number of cycles experienced by the cell before failure. The approach presented now consists in weighting the cycles with respect to their DoD. For each DoD range, the ratio number of operational cycles to number of tested cycles (as given by figure 10) is formed. Then the sum over all DoD ranges is

performed in order to obtain an index, which will be called battery life index in the following. Table 3 presents the battery life index without IPS (38.5 %) and with IPS (44.1 %).

DoD (%)	Life test data	Without IPS		With IPS	
		cycles	life index	cycles	life index
65-70	2300	600	26.1%	600	26.1%
55-65	3700	300	8.1%	300	8.1%
45-55	6500	180	2.8%	180	2.8%
35-45	12000	120	1.0%	210	1.8%
25-35	22500	120	0.5%	575	2.6%
15-25	44500	30	-	855	1.9%
5-15	100000	-	-	825	0.8%
<b>TOTAL</b>	-	1350	<b>38.5%</b>	3545	<b>44.1%</b>

**Table 3: Battery life index with and without IPS**

The increase of the battery life index due to IPS operation is then limited to 5.6 % which has led to the conclusion that the proposed battery utilization is not critical with respect to battery life (an additional year of operation of a conventional 15-year design life spacecraft increases by nearly 7% the battery life index).

### 5.5 IPS accomodation

In a EUROSTAR mechanical architecture (cone-cylinder assembly, four externally mounted chemical propellant tanks), the xenon tanks are implemented in the cone-cylinder with the pressurant tanks. In a central cylinder architecture with internally mounted chemical propellant tanks, the xenon tanks must be implemented outside the central structure on a dedicated support structure.

The UK-10's are implemented in pairs on two modules including the TPM, each module being attached to the spacecraft body via brackets with a geometry compatible with the launcher fairings and the stowed solar array and which maximizes the NSSK thrust efficiency (70%).

Two alternatives are possible regarding the accomodation of the highly dissipative PCCE's. They can be mounted on the heatpipe network of one of the payload radiators. Considering the PCCE efficiency and the rejection capability of a typical payload radiator, the radiator area must be increased by 0.42 m<sup>2</sup>. The drawback of this approach is the slightly increased daily temperature variation of the repeater units as a result of the IPS operation.

The other alternative consists in mounting both units on the North (or South) spacecraft side with a dedicated radiator section, i.e. conductively and radiatively decoupled from the rest of the spacecraft. The thermal capacity of both units can be used to store heat during the maneuver which is rejected in the time interval separating two maneuvers. This approach minimizes the radiator allocation (0.15m<sup>2</sup>) and the heater power (30W) and has therefore been selected.

### 6. Spacecraft design performance

System budgets have been established for an INTELSAT VII-A mission with and without IPS. The launch mass

budget in both cases for a standard Ariane launch is presented in table 4.

	Without IPS	With IPS
Payload	525 kg	525 kg
Structure	216 kg	218 kg
CPS	129 kg	96 kg
IPS	-	68 kg
Power	399 kg	405 kg
TCR	55 kg	55 kg
ADCS	57 kg	75 kg
Thermal	125 kg	125 kg
Electrical integration	102 kg	102 kg
Mechanical integration	64 kg	64 kg
Margins	84 kg	87 kg
Spacecraft dry mass	1756 kg	1820 kg
Chemical propellant	2244 kg	1393 kg
Xenon	-	59 kg
Helium	7 kg	6 kg
Launch mass	4007 kg	3278 kg

**Table 4: Launch mass budget**

**Structure:** Due to the lower launch mass, the mass of the central structure can be significantly reduced (e.g. lateral stiffness significantly lower to insure the same first lateral frequency, load fluxes at the launch vehicle adapter significantly decreased). This is however not taken into account. The xenon tank support structure has been included in the budget.

**CPS:** The CPS is lighter with IPS due to the chemical propellant and pressurant tanks of lower capacity.

**IPS:** The IPS mass budget includes two xenon tanks, four UK-10, two thruster modules and brackets, two PCCE's with thermal hardware, two TSE's, two PSME's, the PSDE, the pipework and the harness.

**Power:** The mass impact on the power subsystem is related to the slightly increased solar array power requirement and to the modifications of the battery thermal control.

**ADCS:** The mass impact is due to the two magnetic bearing wheels (instead of two fixed momentum wheels) and the two TPM's and associated modifications of the spacecraft actuator drive electronics.

**Thermal:** The additional thermal hardware has been budgeted on the IPS side and on the power subsystem side (battery).

Finally the spacecraft dry mass is increased by 64 kg while the launch mass is decreased by 730 kg, taking into account the selected station-keeping strategy. The IPS equipped spacecraft can then be launched by an Ariane 44P booster (instead of Ariane 44LP) with the corresponding launch cost reduction. Propellant budget performed for a Kennedy launch shows that the spacecraft can be launched by an Atlas 2AS booster.

### 7. Benefits evaluation and conclusion

The use of IPS leads to a significant launch cost reduction due to the reduced spacecraft launch mass allowing the use

of less powerful launchers or launcher versions. Considering a 30 000 \$/kg launch cost rate, the launch cost reduction reaches 21.8 M\$. Obviously the recurring cost of IPS and its implementation on the spacecraft slightly decreases the above figure but in the proposed spacecraft design, this is limited to a minimum. The use of IPS also maintains the Atlas compatibility for a larger range of payload.

Furthermore the following additional benefits offered by the proposed IPS equipped spacecraft have been identified:

- Enhancement by 0.02° of the antenna pointing accuracy
- Improvement of the station-keeping accuracy and/or autonomy allowing a significant decrease of large fleet control centre work load and simple collocation of several spacecraft within a +/- 0.05° orbital slot.
- Decrease of outage risk and duration as a result of the low thrust maneuvers.

In the proposed spacecraft design, the impacts on the power and thermal subsystems are minimum and acceptable. The proposed ion thruster arrangement also minimizes the impact on the spacecraft environment so that no detrimental effects on the payload operation and on the solar array degradation are expected.

**Acknowledgements:**

The authors wish to acknowledge B. Free, A. Sitapara and J. Owens of INTELSAT for their helpful contribution as well all the MMS engineers who have participated to this study.

This paper is based on work performed, in part, under the sponsorship and technical direction of the International Telecommunication Organisation (INTELSAT).

**References**

- 1 "The INTELSAT VII-A spacecraft"; P. Neyret et al; AIAA-92-1946-CP.
- 2 "A new three-axis control system for a geosynchronous satellite in transfer orbit"; A. Benoit;
- 3 "Benefits of electric propulsion for orbit injection of communications spacecraft"; F. Porte et al; AIAA-92-1955.
- 4 "ATS-6 Final Engineering Performance Report"; Volume 2; NASA-1080; 1981.
- 5 "Advanced spacecraft concepts using electric propulsion"; M. Perdu; AIAA-92-3513.
- 6 "The low noise momentum wheel MW-X EM design and predicted properties"; T. Eckardt.
- 7 "Modeling performance degradation in Nickel Hydrogen cells"; L.H. Thaller et al; Proceeding of the European Space Power conference; Florence September 1991; ESA-SP-320.

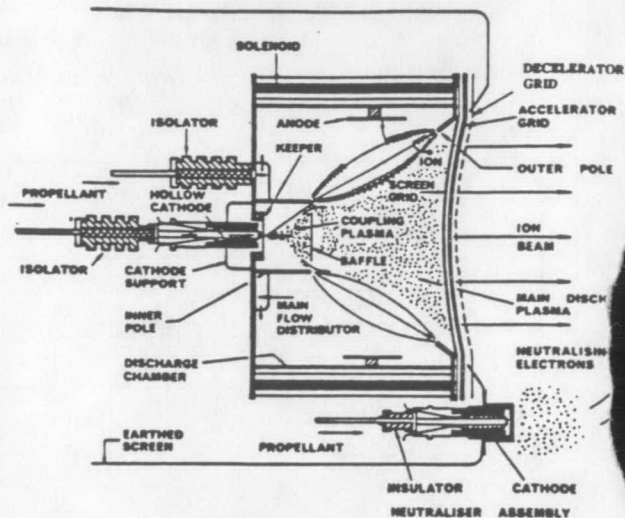


Figure 1 UK-10 schematic

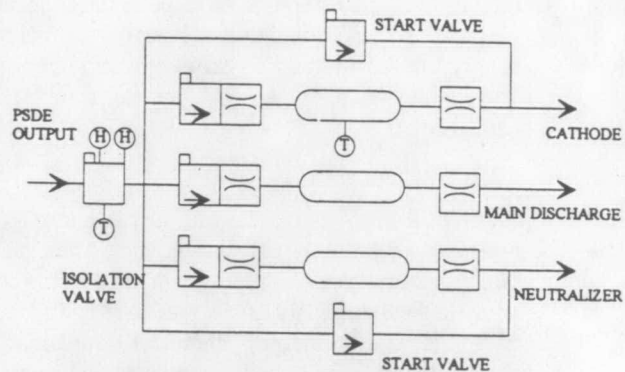


Figure 2 PSME schematic

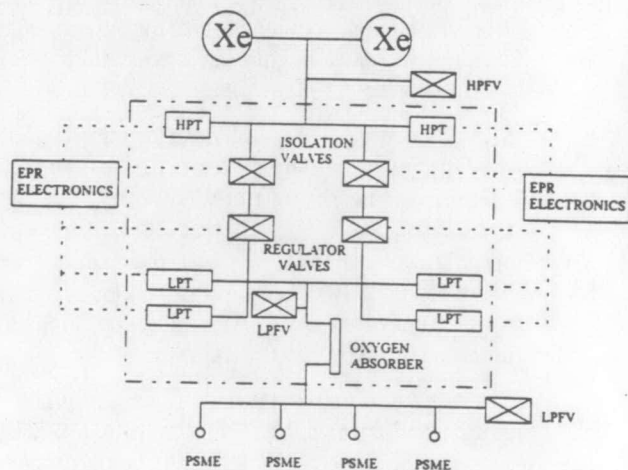


Figure 3 PSDE schematic

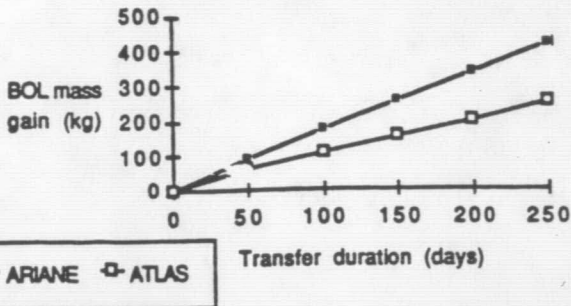


Figure 4 BOL mass gains (orbit insertion with IPS)

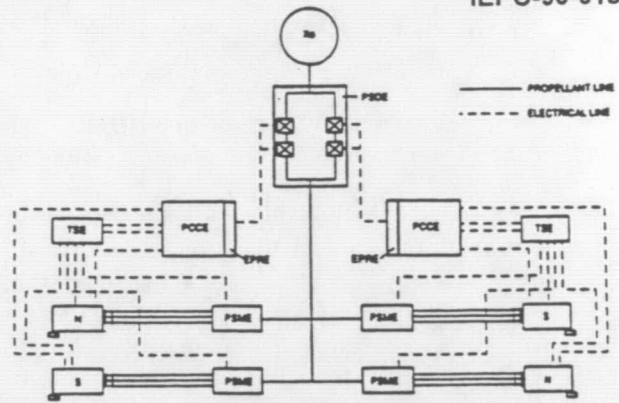
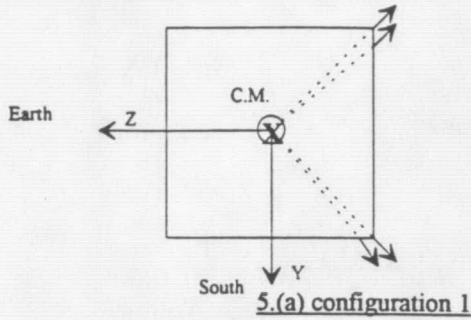
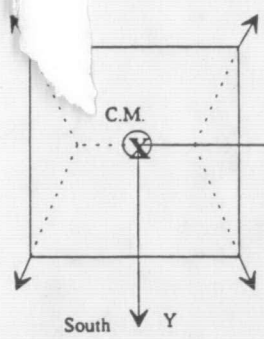


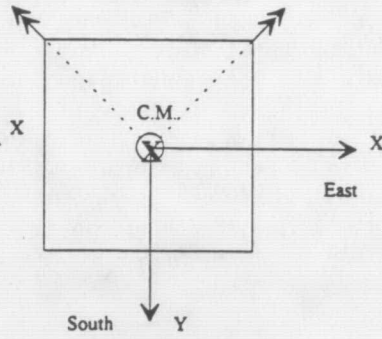
Figure 7 IPS schematic



5.(a) configuration 1



5.(b) configuration 2.1



5.(c) configuration 2.2

Figure 5 Candidate thruster configurations

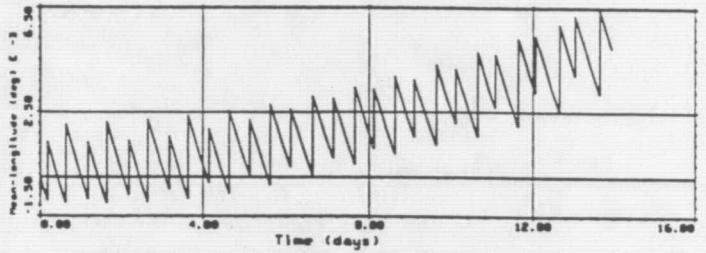


Figure 8 Mean longitude evolution over a 2-week maneuver cycle

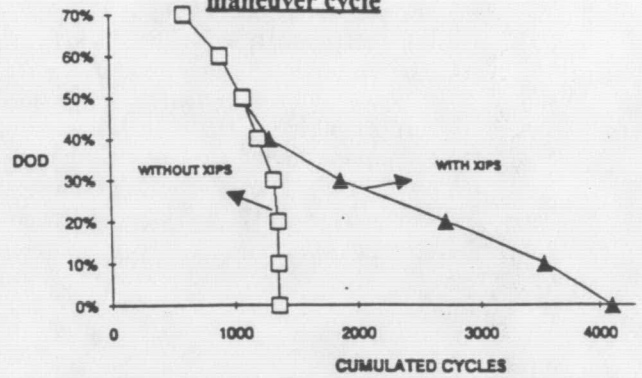
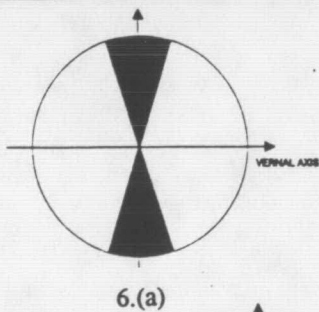
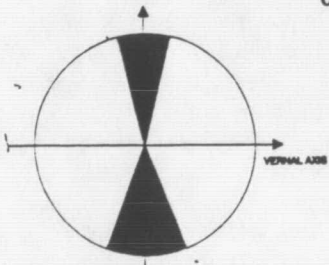


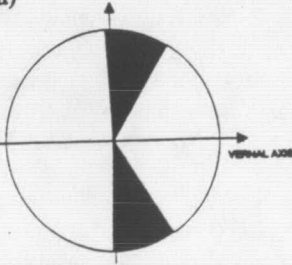
Figure 9 Battery cycling with and without IPS



6.(a)



6.(b)



6.(c)

Figure 6 Combined inclination-eccentricity correction

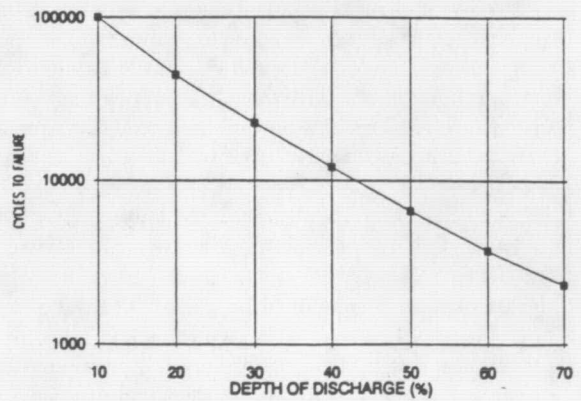


Figure 10 Battery life test data envelope